Korean J. Chem. Eng., **23**(1), 43-56 (2006)

Application of computational fluid dynamics analysis for improving performance of commercial scale selective catalytic reduction

Jin Man Cho†, Jeong-Woo Choi*, Sung Ho Hong, Kwang Chu Kim**, Jung Hee Na** and Jun Yub Lee****

Department of Chemical & Biomolecular Engineering,
*Department of Chemical & Biomolecular Engineering and Interdisciplinary Program of Integrated Biotechnology, Sogang University, #1 Sinsu-dong, Mapo-gu, Seoul 121-742, Korea
**Korea Power Engineering Company, INC. 360-9 Mabuk-ri, Guseong-eup, Yongin-si, Gyeonggi-do 449-713, Korea
(*Received 28 February 2005 • accepted 8 August 2005*)

Abstract–The performance of commercial scale selective catalytic reduction (SCR) system is strongly dependant upon the degree of mixing between NH_3 and NOx or NH_3 concentration distribution at the catalyst layer according to the reaction kinetics of SCR catalysts. Insufficient mixing of the reduction agent and NOx mass flow necessitates an uneconomically large catalyst volume and high NH_3 slip to meet the required NOx emission values. The effective methodology which can increase the performance of commercial scale SCR through improving NH_3 concentration distribution at the catalyst layer using computational fluid dynamics (CFD) analysis was suggested and applied to the real operations. The operation results have shown that the performance of commercial SCR was improved from 54.4% to 74.8% as NH_3 concentration deviation at the catalyst layer was reduced from 23.6% to 8.6%. It is established that the increase of NH_3 concentration uniformity at the catalyst layer contributes to improvement of performance of commercial scale SCR.

Key words: Commercial Scale Selective Catalytic Reduction, Computational Fluid Dynamics, NOx, NH_3 Concentration Distribution

INTRODUCTION

Various NOx treatment systems for pollution sources such as industrial plants and power plants have been installed to meet the reinforced restriction and limitation for atmospheric pollutants. Selective catalyst reduction (SCR) is an effective treatment system used worldwide for large-scale plants [Arbind, 1995; Bruce, 1995; Jaime, 1993; Kotter and Lintz, 1991]. The performance of an SCR system depends on the catalysts and the operation parameters. SCR operating parameters are reaction temperature, space velocity (SV), flue gas components, NH_3/NOx molar ratio, the limitation of NH_3 slip, SCR operation time and the degree of mixing between NH_3 and NOx or NH_3 distribution at the catalyst layer [Ralf et al., 2003]. Except for the degree of mixing between NH_3 and NOx or NH_3 distribution, other operation parameters of existing SCR systems are restricted in improving or modifying because those need additional costs and bring about a drop in efficiency of existing main plants and there are many limitations in retrofitting. The degree of mixing between NH_3 and NOx or NH_3 concentration distribution has a margin for improvement in a large-scale SCR system. According to the reaction kinetics of SCR catalysts, the effectiveness of the SCR process is strongly dependent upon the degree of mixing between NH_3 and NOx or NH_3 concentration distribution at the catalyst layer [Freek et al., 1993; Jiri et al., 1993]. Insufficient mixing of the reducing agent and NOx mass flow necessitates an uneconomically large catalyst volume and high NH_3 slip to meet the required NOx emission values. The static mixer at downstream of ammonia injection grid (AIG) and guide vanes at upstream of catalyst layer as a flow correction device are installed in the coal fired power plant in order to obtain the uniform NH_3 concentration distribution at the catalyst layer [Heck et al., 1994; Kenneth and John, 1993; Kevin et al., 1999]. The combined cycle power plant does not need additional SCR reactor because catalyst layer and AIG should be installed inside heat recovery steam generators (HRSG). In addition, it is difficult to install flow correction devices because those cause additional pressure drop to reduce the efficiency of power generation [Kokkinos et al., 1999]. In general, an SCR system in combined cycle power plant should obtain uniform NH_3 concentration distribution at the catalyst layer without additional flow correction devices. Therefore, it is important to find the optimal AIG location, where flue gas behavior is uniform, in order to obtain a uniform NH_3 concentration distribution at the catalyst layer. The flue gas behavior in HRSG becomes uniform during passing through heat pipe bundles. The catalyst layer should be installed in the region in the middle region of heat pipe bundles. In many cases, the AIG is installed in HRSG inlet expansion duct region, which has non-uniform flue gas behavior. In these cases, it is difficult to get the uniform NH_3 concentration distribution at the catalyst layer.

In this study, an effective methodology which can increase the performance of commercial scale SCR in combined cycle power plant was suggested and applied to real operations. An analytic method using computational fluid dynamics (CFD) was introduced. Flue gas mass fluxes passing through individual AIG groups were calculated by CFD analysis. And the optimal NH_3 feed rates for individual AIG groups to form the uniform NH_3 concentration distribution at the catalyst layer were determined according to the flue gas mass fluxes. In the course of CFD analysis, NH_3 concentration deviation, D_c at the catalyst layer was defined and calculated for all cases of experiments in order to analyze the relationship with NOx

†To whom correspondence should be addressed.
E-mail: zozinman@mobis.co.kr

Table 1. Catalyst specifications

Type	Honeycomb	Production method		Extrusion
Number of cells (CPSI)	35	Perforation ratio (%)		≥72
Length (mm)	140±2/550±2	Torsion (mm)	&1	≤1.3
Outer length (mm)	150±2		&2	≤1.5
Thickness of outer wall (mm)	≤1.3	Contact area (m^2/m^3)		≥792
Thickness of inner wall (mm)	0.65±0.05	Bulk density (kg/m^3)		550±2

removal efficiency.

EXPERIMENTAL APPARATUS AND PROCEDURE

1. SCR Catalyst

The specifications of the extruded honeycomb catalyst used in this study are described in Table 1. It consists of TiO_2/Mn oxides. The catalyst elements are combined into carbon steel boxes called modules, which are designed primarily with a view to permanently ensuring an operationally suitable arrangement of the catalysts in the reactor.

2. Commercial Scale SCR

The commercial scale SCR system is installed in horizontal type heat recovery steam generator (HRSG) of a combined cycle power plant. It consists of NH_3 unloading and storage part, NH_3 injection part and SCR catalyst layer and accessories part. The system configuration is shown in Fig. 1. The flue gas flow rate is 800,000 Nm^3/hr (based on standard of design). The catalyst layers consist of two layers, 1st catalyst layer (22 m^3) and 2nd catalyst layer (44 m^3). And 1st catalyst layer has two sub-layers, which have 11 m^3 of catalyst, respectively. The total volume of catalyst is 66 m^3. Therefore, SV of commercial scale SCR is 12,121 hr^{-1}. Fig. 2 shows the location of catalyst layers and their specification. Fig. 3 shows AIG in commercial scale SCR.

3. Procedure

3-1. Performance Tests Using Individual AIG Group

The objective of this test is to investigate the flue gas mass flux behavior in HRSG and the relationship between performance and NH_3 concentration deviation experimentally. NH_3 gas was allowed to feed from only one AIG group for each test. Duration for each test was 30 minutes after previous operation for 30 minutes to stabilize the SCR system, and inlet NOx, outlet NOx concentration and NH_3 slip were monitored at one minute intervals. Total NH_3 feed rate was maintained constantly by setting NH_3 gas flow control valve during the period of whole tests.

3-2. Performance Tests Using All AIG Groups

The performance test operations using all AIG groups were implemented in order to evaluate effectiveness of the proposed method which can form the uniform NH_3 concentration distribution at the catalyst layer using CFD analysis. The number of operation cases is four. The first case experiment is to apply the same NH_3 feed rate for all AIG's groups. And the other experiments are to apply different NH_3 feed rates for individual AIG's groups, which were determined based on flue gas mass flux passing through individual AIG groups obtained from CFD analysis result. In these tests, SCR control system logic was set up to let NH_3 slip to be maintained at 10 ppm and the total NH_3 feed rate was controlled automatically according to inlet NOx concentration. For each case, twice opera-

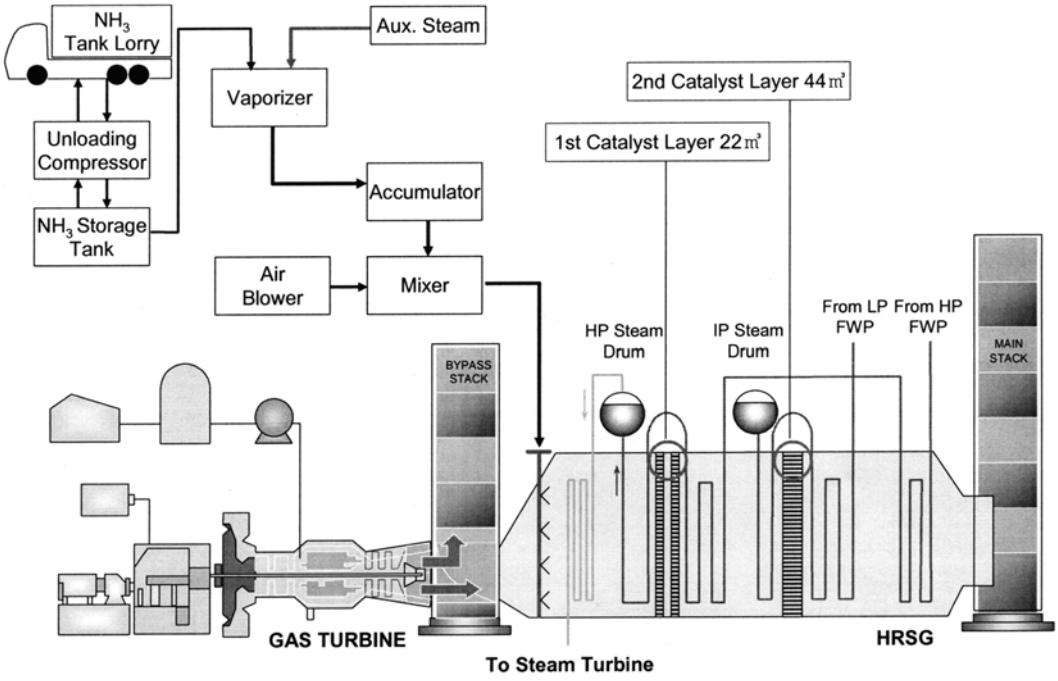

Fig. 1. Commercial scale SCR system configuration.

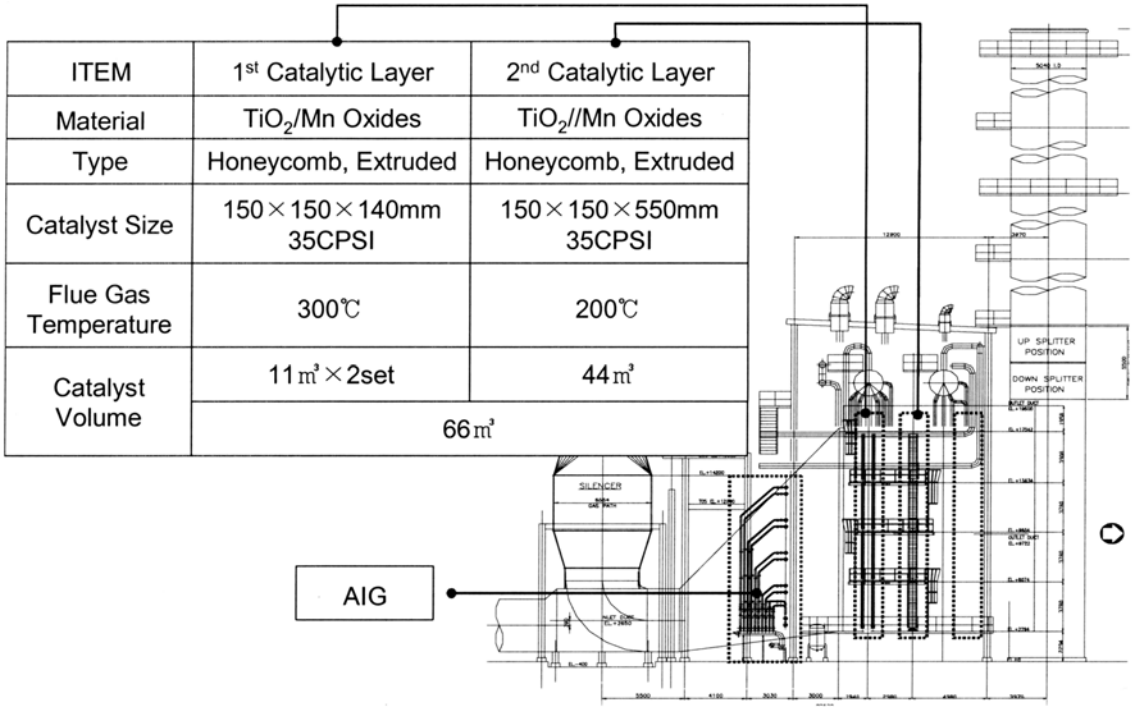

Fig. 2. The catalyst layers in commercial scale SCR system.

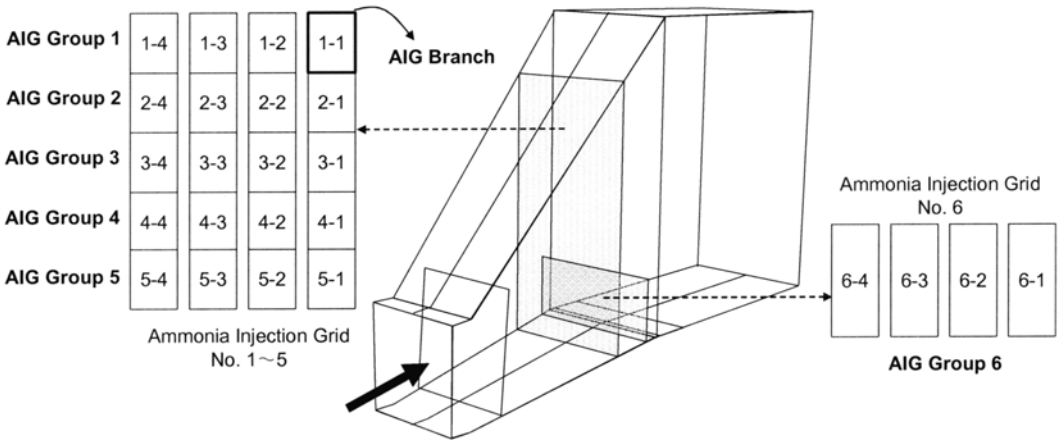

Fig. 3. Ammonia injection grid groups and branches of commercial scale SCR.

tions were implemented and each operation was maintained for 2 hours. Inlet NOx, outlet NOx concentration and NH_3 slip were also measured at one minute intervals.

COMPUTATIONAL FLUID DYNAMICS ANALYSIS

1. CFD Analysis for Commercial Scale SCR in HRSG

Computational domain for fluid dynamics calculation is defined. The governing equations for physical properties such as velocity, pressure and temperature are derived by means of applying mass, momentum and energy conservation theory. However, it is impossible to obtain an analytic solution by manual calculation method no matter how simple the case is because these are non-linear partial derivative equations. Therefore, computational fluid dynamics analysis method has been introduced as an alternative [Adams et al., 2002; Kevin et al., 2000; Sayre and Milobowski, 1999].

The existing plants such as thermal power plants and incinerators which need SCR system have expansion or reduction section due to catalyst layer, AIG, bypass duct installation in course of retrofitting. Especially, it is necessary to equip with catalyst layers and AIG into HRSG in case of a combined cycle power plant; thus, flue gas behavior passing through the catalyst layer must be changed by inlet expansion duct, flow correction devices and heat pipe bundles. It is necessary to determine the optimal location of AIG, to equip with additional guide vanes or to regulate NH_3 feed rates of individual AIG branches for a uniform NH_3 concentration distribution at the catalyst layer. A physical model test or numerical analysis can be used to predict the result of these modification.

2. Governing Equations

The following are mass, momentum and scalar conservation equa-

tions.

Mass Conservation

$$\frac{\partial \rho}{\partial t} + \frac{\partial (\rho u_j)}{\partial x_j} = S_m \tag{1}$$

Momentum Conservation

$$\frac{\partial (\rho u_i)}{\partial t} + \frac{\partial (\rho u_i u_j)}{\partial x_j} = -\frac{\partial p}{\partial x_i} + \frac{\partial}{\partial x_j}\left[\mu\left(\frac{\partial u_i}{\partial x_j} + \frac{\partial u_j}{\partial x_i}\right)\right] + \rho g_i + F_i \tag{2}$$

Scalar Conservation

$$\frac{\partial (\rho \phi)}{\partial t} + \frac{\partial (\rho u_i \phi)}{\partial x_j} = \frac{\partial}{\partial x_j}\left(\Gamma \frac{\partial \phi}{\partial x_j}\right) + S_\phi \tag{3}$$

3. Finite Volume Element Method [Pantankar, 1980]

Discretization of governing equations is as follows. For one dimensional system and steady state, scalar ϕ conservation equation is given as Eq. (4).

$$\frac{\partial (\rho u \phi)}{\partial x} = \frac{\partial}{\partial x}\left(\Gamma \frac{\partial \phi}{\partial x}\right) + S_\phi \tag{4}$$

For one cell, by integrating Eq. (4) and applying divergence theorem, convection term of the left side is changed into Eq. (5).

$$\int_{Volume\ V} \frac{\partial (\rho u \phi)}{\partial x} dV = \int_{surface\ A} \rho u \phi \, dA = (\rho u \phi A)_e - (\rho u \phi A)_w \tag{5}$$

Diffusion term and source term of the right side are changed into Eq. (6).

$$\int_{volume\ V}\left[\frac{\partial}{\partial x}\left(\Gamma \frac{\partial \phi}{\partial x}\right) + S_\phi\right] dV = \left(\Gamma \frac{\partial \phi}{\partial x} A\right)_e - \left(\Gamma \frac{\partial \phi}{\partial x} A\right)_w + S_\phi \Delta V \tag{6}$$

The value of ϕ and $\partial\phi/\partial x$ at locations between one cell and neighbor cell should be calculated in the center because all variables are stored in the center of cell. First order upwind scheme, power-law scheme and second order upwind scheme are used in calculating these values [Fluent User's Guide, 1996]. By means of calculating Eq. (6) for each cells and combining, Eq. (7) as a matrix equation can be obtained.

$$a_P \phi_P = \sum_{nb} a_{nb} \phi_{nb} + b \tag{7}$$

where, nb is neighbor cells of one cell. In case of two dimensional rectangular mesh the number of neighbor cells is four and in case of three dimensional system it is six. As a_p and a_{nb} are the function of ϕ, the solution for non-linear equation can be obtained by iteration method.

4. SIMPLE Algorithm and Numerical Schemes

The pressure correction equation of simple-implicit method for pressure-linked equation (SIMPLE) algorithm used in FLUENT™ is obtained from modifying mass and momentum conservation equations. The mass and momentum equations should be calculated in order to analyze flue gas behavior and the transfer equation for 1 chemical species should be calculated in order to analyze the injected air and the NH_3 concentration distribution. Standard k-ε model [Launder and Spalding, 1972] is used as a turbulence model. The density is obtained from volume ratio of each chemical species and temperature. The values for average temperature at the region of calculation are adopted as other physical properties.

5. Meshes

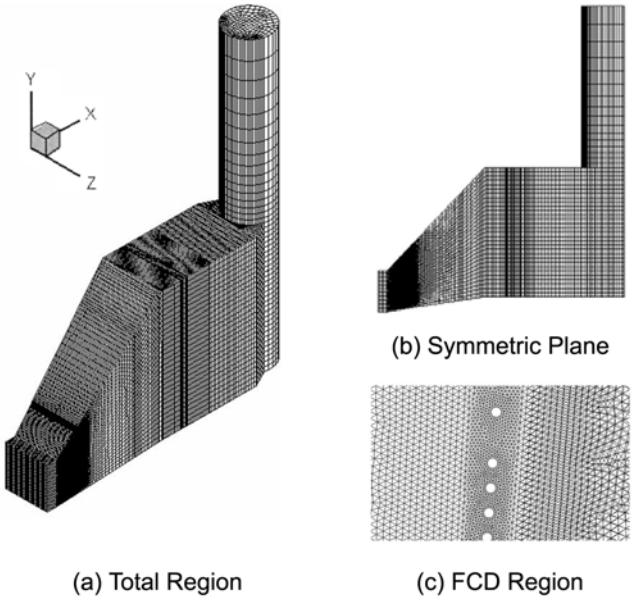

Fig. 4. Meshes for CFD analysis.

Fig. 4 shows meshes for analyzing flue gas behavior and NH_3 concentration distribution in commercial scale SCR. CFD analysis was done for half of the total region because horizontal HRSG is a symmetric structure. The meshes consist of about 200,000 hexahedral and pentahedral cells and are clustered near wall, porous media and FCD region to increase accuracy.

6. Porous Media

HRSG consists of several heat exchangers which have numerous heat pipe bundles. The meshes should be prepared according to the real shapes of pipe bundles and they should be included in calculation for complete analysis. However, it is impossible to calculate in considering present computer ability. Therefore, the regions of heat pipe bundles and catalyst layer are considered as porous media in this study. To verify the feasibility for porous media assumption CFD analysis was implemented for three cases which have different resistance coefficients in heat pipe bundles such as $C_v=C_h$, $C_v=0.5C_h$ and $C_v=0.1C_h$. C_v is vertical direction (Y-axis) resistance coefficient and C_h is horizontal direction (X-axis) resistance coefficient. However, flue gas cannot flow toward vertical direction in the catalyst layer because the catalyst is honeycomb type.

In CFD analysis, numerical approach for porous media is treated as momentum source term of general fluid flow equation and this source term consists of viscous loss term and inertial loss term based on Darcy's law.

$$S_i = \nabla p = \sum_{j=1}^{3} D_{ij} \mu V_j + \sum_{j=1}^{3} C_{ij} \frac{1}{2} \rho |V_j| V_j \tag{8}$$

Calculating the source term determines the pressure drop in the porous region and the pressure drop is proportional to fluid velocity in cells.

In case of simple porous media which has the same value for X, Y and Z direction, Eq. (8) can be simplified like Eq. (9).

$$\nabla p = \frac{\mu}{\alpha} V_i + C_2\left(\frac{1}{2} \rho |V_i| V_i\right) \tag{9}$$

In general, it is not necessary to consider permeability in case of pipe bundles and porous plate; thus, only C_2 should be calculated and it can be obtained from Eq. (10).

$$C_2 = \frac{K_L'}{T} \tag{10}$$

The relationship between K_L' and K_L can be given such as Eq. (11) in case of full opening.

$$K_L' = K_L\left(\frac{V^2_{actual\ open}}{V^2_{100\%\ open}}\right) = K_L\left(\frac{A_{actual\ open}}{A_{100\%\ open}}\right) \tag{11}$$

In case of 100% opening, K_L can be obtained from Eq. (12)

$$K_L = \frac{\Delta p}{\frac{1}{2}\rho V^2} \tag{12}$$

7. CFD Analysis for Flue Gas Behavior

Average flue gas mass flux, ρV_x passing through the AIG is calculated from the result of CFD analysis. It can be considered as NOx amount which should react with NH_3 because NOx concentration is a constant value in flue gas. Therefore, NH_3 feed rates for individual AIG groups can be determined based on average flue gas mass flux passing through the AIG. And also D_m as a flue gas distribution deviation parameter in Eq. (13) is introduced to evaluate the uniformity of flue gas behavior. D_m is calculated at AIG and catalyst layers.

$$D_m = \sqrt{\left(\frac{\int(\rho w - \overline{\rho w})^2 dA}{A}\right)} / \sqrt{\rho w} \times 100\% \tag{13}$$

8. CFD Analysis for NH_3 Concentration Distribution

CFD analysis for NH_3 concentration distribution was implemented for all operation cases assuming the ratio of resistance coefficients is C_v=0.5C_h. NH_3 concentration distribution deviation parameters (D_c) for total region including catalyst layer are calculated. The homogeneity of NH_3 concentration at the catalyst layer can be evaluated from D_c. D_c is defined as Eq. (14) and the relationship between D_c and the performance of commercial scale SCR was analyzed.

$$D_c = \sqrt{\left(\frac{\int(c - \overline{c})^2 dA}{A}\right)} / \sqrt{c} \times 100\% \tag{14}$$

RESULTS AND DISCUSSION

1. CFD Analysis

1-1. Temperature and Pressure Distribution inside HRSG

Fig. 5 shows the flue gas temperature distribution of HRSG equip-

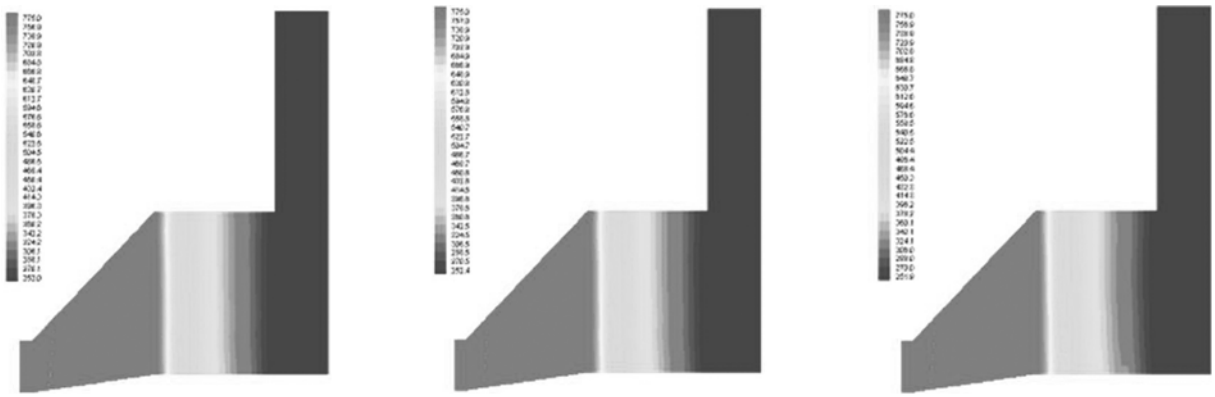

Fig. 5. CFD analysis result for flue gas temperature distribution (^oK) at the HRSG symmetric plane.

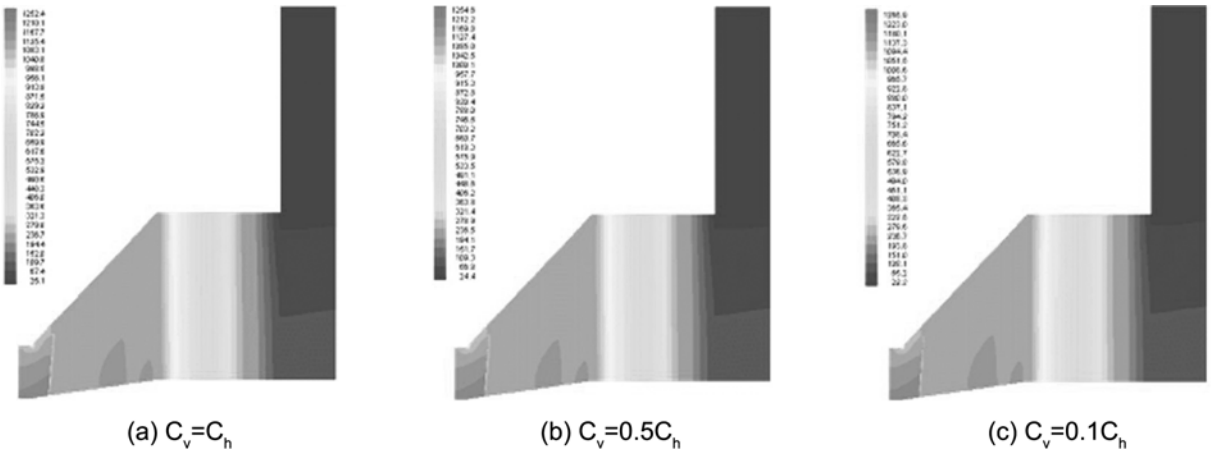

Fig. 6. CFD analysis result for flue gas pressure distribution (mmH_2O) at the HRSG symmetric plane.

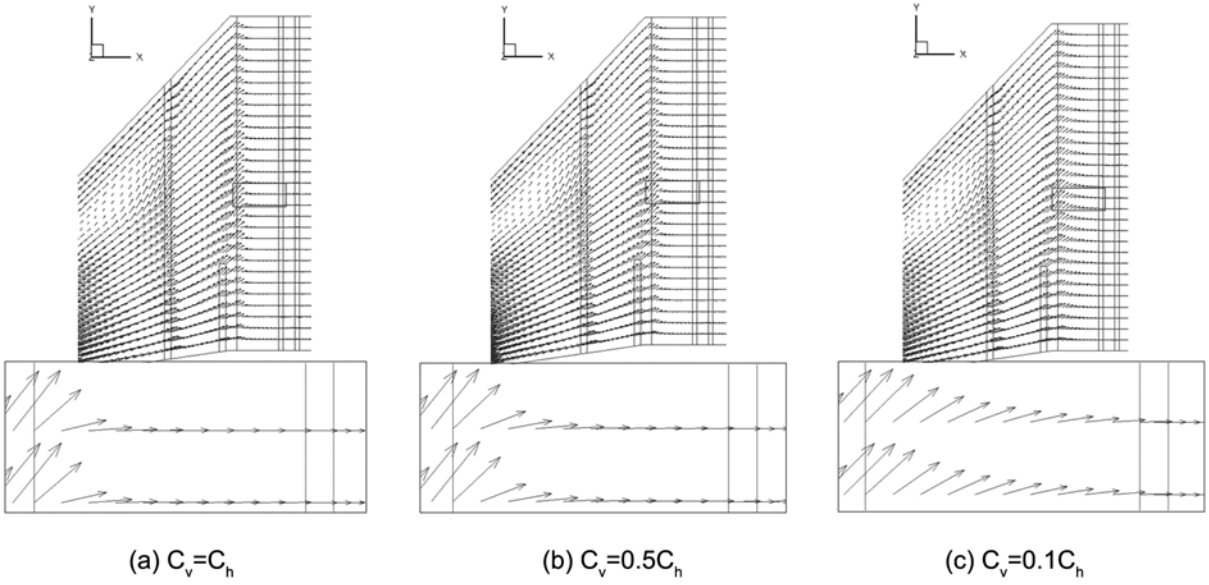

Fig. 7. Velocity vector in AIG and catalyst layer region.

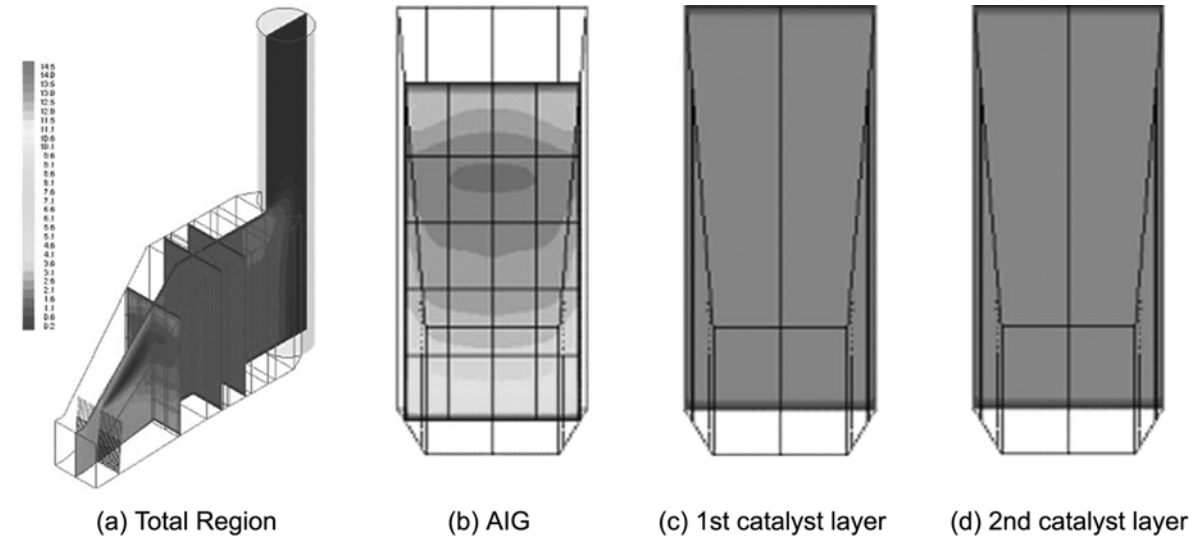

Fig. 8. Flue gas mass flux, ρV_x (kg/m^2·sec) distribution for $C_v=C_h$.

ped with commercial scale SCR for $C_v=C_h$, $C_v=0.5C_h$ and $C_v=0.1C_h$. Temperature is decreased by heat exchange between flue gas and heat pipe bundles as flue gas flows toward the stack. Fig. 6 shows the flue gas pressure distribution of HRSG for $C_v=C_h$, $C_v=0.5C_h$ and $C_v=0.1C_h$. And also pressure is decreased by pressure drop due to heat pipe bundles and catalyst layers.

1-2. Flue Gas Behavior

Fig. 7(a), (b) and (c) show flue gas velocity vector plots at the symmetric plane for $C_v=C_h$, $C_v=0.5C_h$ and $C_v=0.1C_h$, respectively. It can be seen that there is rapid upward flow (V_y) around the first heat exchanger, high pressure superheater (HPSH) and this leads to uniform flue gas flowing in the downstream region. It can be observed that as the vertical resistance coefficient becomes smaller, the upward flow of flue gas is stronger in the HPSH region. The upward flow of flue gas of the low part of HRSG is stronger than that of the upper part of HRSG. After passing through HPSH, the main flowing direction velocity (V_x) becomes dominant and the other direction velocities (V_y, V_z) become tiny. Figs. 8, 9 and 10 show flue gas mass flux, ρV_x distribution for $C_v=C_h$, $C_v=0.5C_h$ and $C_v=0.1C_h$, respectively. It shows that as flue gas flows toward stack its distribution becomes uniform. Table 2 shows V_x, ρV_x and ρV_x deviation D_m for $C_v=C_h$, $C_v=0.5C_h$ and $C_v=0.1C_h$. Fig. 11 shows variation of D_m values at AIG, 1st catalyst layer and 2nd catalyst layer for $C_v=C_h$, $C_v=0.5C_h$ and $C_v=0.1C_h$. D_m values are decreased as flue gas flows toward stack. As C_v becomes smaller, the upward flow of flue gas has a tendency to be stronger and D_m at the same location is increased. The range of D_m at the AIG for $C_v=C_h$, $C_v=0.5C_h$ and $C_v=0.1C_h$ is 24.3-25.8% and it is much greater than that of D_m at the catalyst layers. It means that flue gas behavior at catalyst layer is more uniform than that at the AIG.

Compared with the amount of flue gas, the amount of NH_3 gas with air injected into HRSG through the AIG is very small. There-

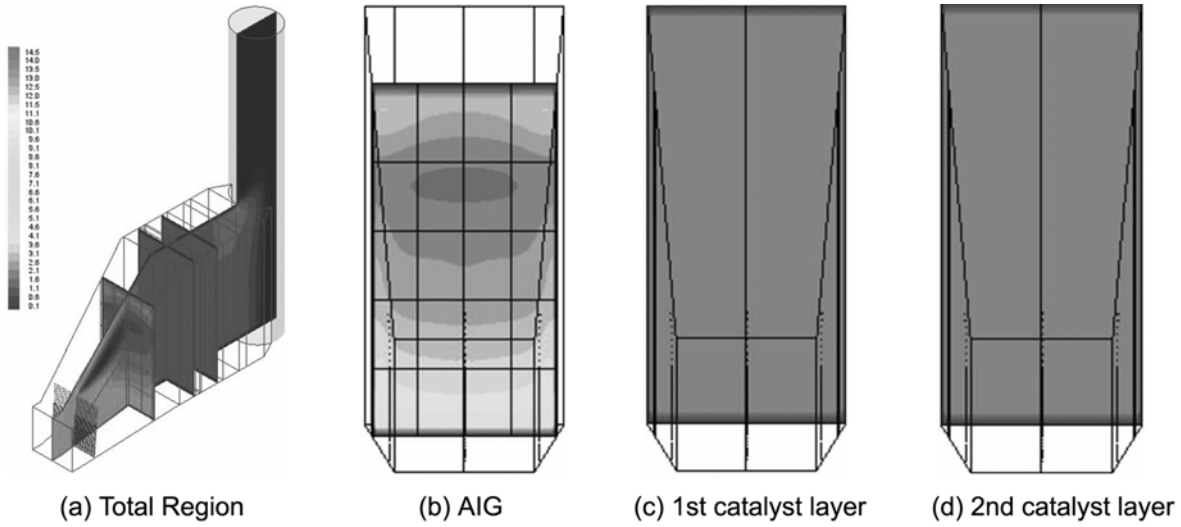

Fig. 9. Flue gas mass flux, ρV_x (kg/m^2·sec) distribution for $C_v=0.5C_h$.

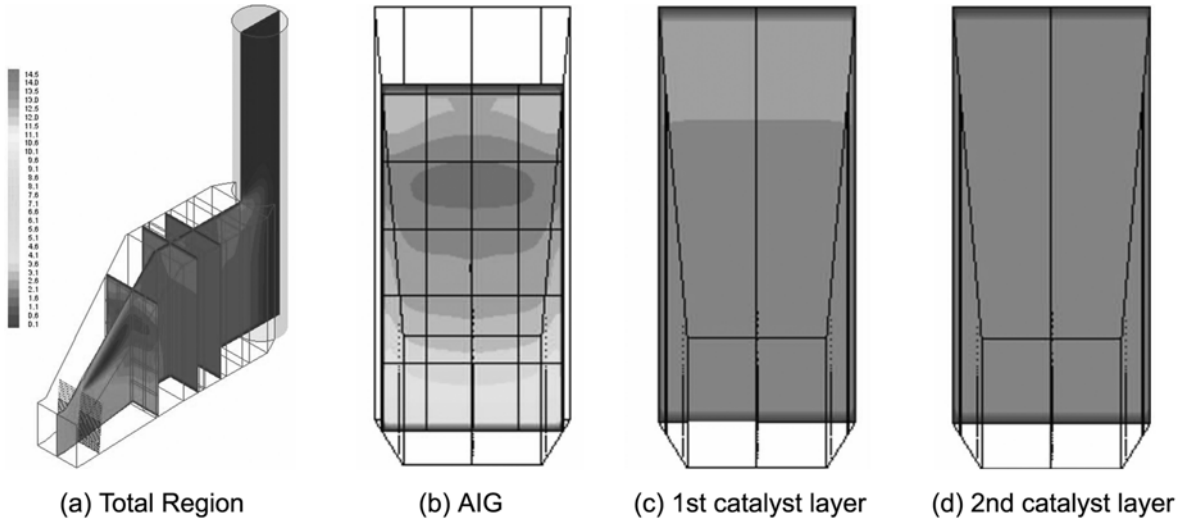

Fig. 10. Flue gas mass flux, ρV_x (kg/m^2·sec) distribution for $C_v=0.1C_h$.

Table 2. CFD result for flue gas velocity (V_x), mass flux (ρV_x) and mass flux deviation (D_m) in horizontal type HRSG

Location	Item	$C_v=C_h$	$C_v=0.5C_h$	$C_v=0.1C_h$
AIG	V_x (m/sec)	6.10	6.10	6.10
	ρV_x (kg/m^2·sec)	2.68	2.68	2.68
	D_m (%)	24.28	24.63	25.76
1st	V_x (m/sec)	3.20	3.20	3.20
Catalyst	ρV_x (kg/m^2·sec)	2.09	2.09	2.09
Layer	D_m (%)	0.31	0.26	1.40
2nd	V_x (m/sec)	2.33	2.33	2.33
Catalyst	ρV_x (kg/m^2·sec)	2.09	2.09	2.09
Layer	D_m (%)	0.32	0.37	0.59

fore, the behavior of NH_3 gas with air is strongly dependent upon that of flue gas inevitably. If the same amount of NH_3 with air for all AIG groups is injected, uneven NH_3 concentration distribution will be formed at the catalyst layer due to deviation of flue gas mass flux. This brings deterioration of performance and increase of NH_3 slip. Therefore, if there is deviation of flue gas mass flux passing the AIG, it is important to determine the NH_3 feed rates for individual AIG groups considering flue gas mass flux in order to form a uniform NH_3 concentration at the catalyst layer and to improve performance of SCR.

1-3. Determination of NH_3 Feed Rates for Individual AIG Groups

Determination of optimal NH_3 feed rates for individual AIG branches can be done by considering flue gas mass flux passing through AIG. They are proportional to magnitudes of flue gas mass flux passing through the individual AIG branches. The flue gas mass flux was calculated by using CFD analysis at $C_v=0.5C_h$ as an average behavior of flue gas. There is little difference between optimal NH_3 feed rates for individual AIG branches based on flue gas mass flux and the values in real operations of commercial scale SCR because of minimum control limit of NH_3 feed rate control valve. Four cases were prepared to apply for performance tests. CASE1 is to apply

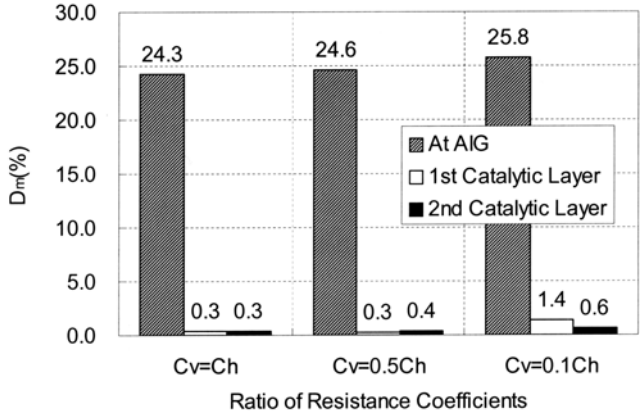

Fig. 11. Flue gas mass flux deviations for $C_v=C_h$, $C_v=0.5C_h$ and $C_v=0.1C_h$: (▨) at AIG; (□) 1st catalyst layer; (■) 2nd catalyst layer.

the same feed rate of NH_3 for all AIG branches and it is prepared to compare with other three cases to apply different NH_3 feed rates considering the flue gas mass flux deviation. In CASE2, the 1st-5th AIG groups are operated without 6th AIG group, whereas all AIG groups are operated in CASE3 and CASE4. However, NH_3 feed rate through the 6th AIG group for CASE3 and CASE4 is different. In CASE3, it is maximum feed rate to be injected through the 6th AIG group's pipe lines. In CASE4, NH_3 feed rate through the 6th AIG group is reduced to 33% of that in CASE3. NH_3 mass flow rates for each CASE are shown in Fig. 12.

2. Performance Tests Using Individual AIG Groups

Fig. 13 shows the CFD analysis results of NH_3 concentration distribution in case of individual AIG group operations. It shows that NH_3 concentration distribution and 1st catalyst area to be supplied with NH_3 are changed by NH_3 injection position. As shown in Table 3 and Fig. 14, there was much difference in NOx removal efficiencies and NH_3 slips although total NH_3 feed amounts for individual tests were almost the same. NOx removal efficiency has a tendency to be decreased as NH_3 slip becomes increased. It is a conflicting result in comparison with general catalyst properties. Fig. 15 shows the relationship between ρV_x at individual AIG groups and D_c at the 1st catalyst layer. It is shown that D_c is inversely proportional to ρV_x except for 1st AIG group, that is, when NH_3 was injected in heavy flue gas flowing region (4th and 5th AIG operations), NH_3 concentration distribution became relatively even at the catalyst layer and NOx removal efficiency was improved as shown in Fig. 16 and Fig. 17.

The main reason for these results can be explained by flue gas mass flux deviation at the AIG position and flue gas correction effect. If NH_3 is injected at the region, at which flue gas mass flux is high, some of the flue gas with NH_3 will be mixed with the flue gas without NH_3 by flue gas rising movement in front of the high pressure superheater. Thus, NH_3 can be supplied to more expanded

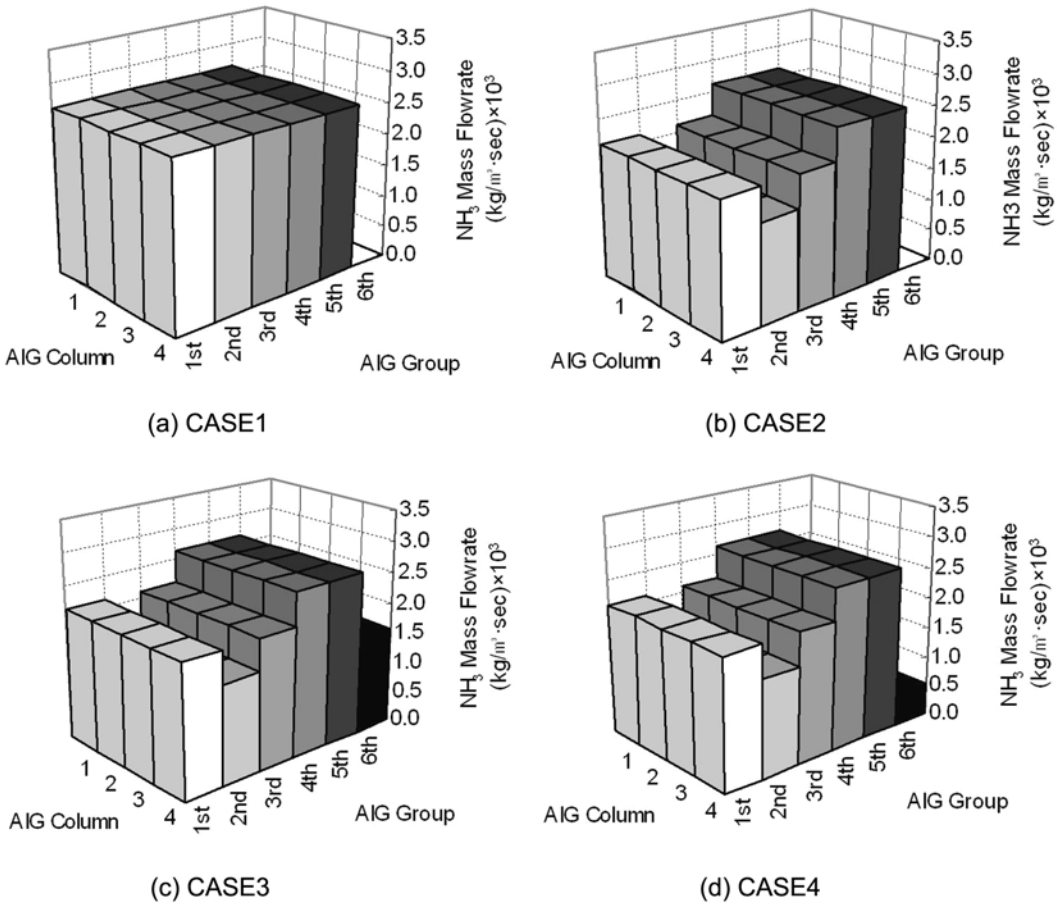

Fig. 12. NH_3 mass flowrates for individual AIG branches.

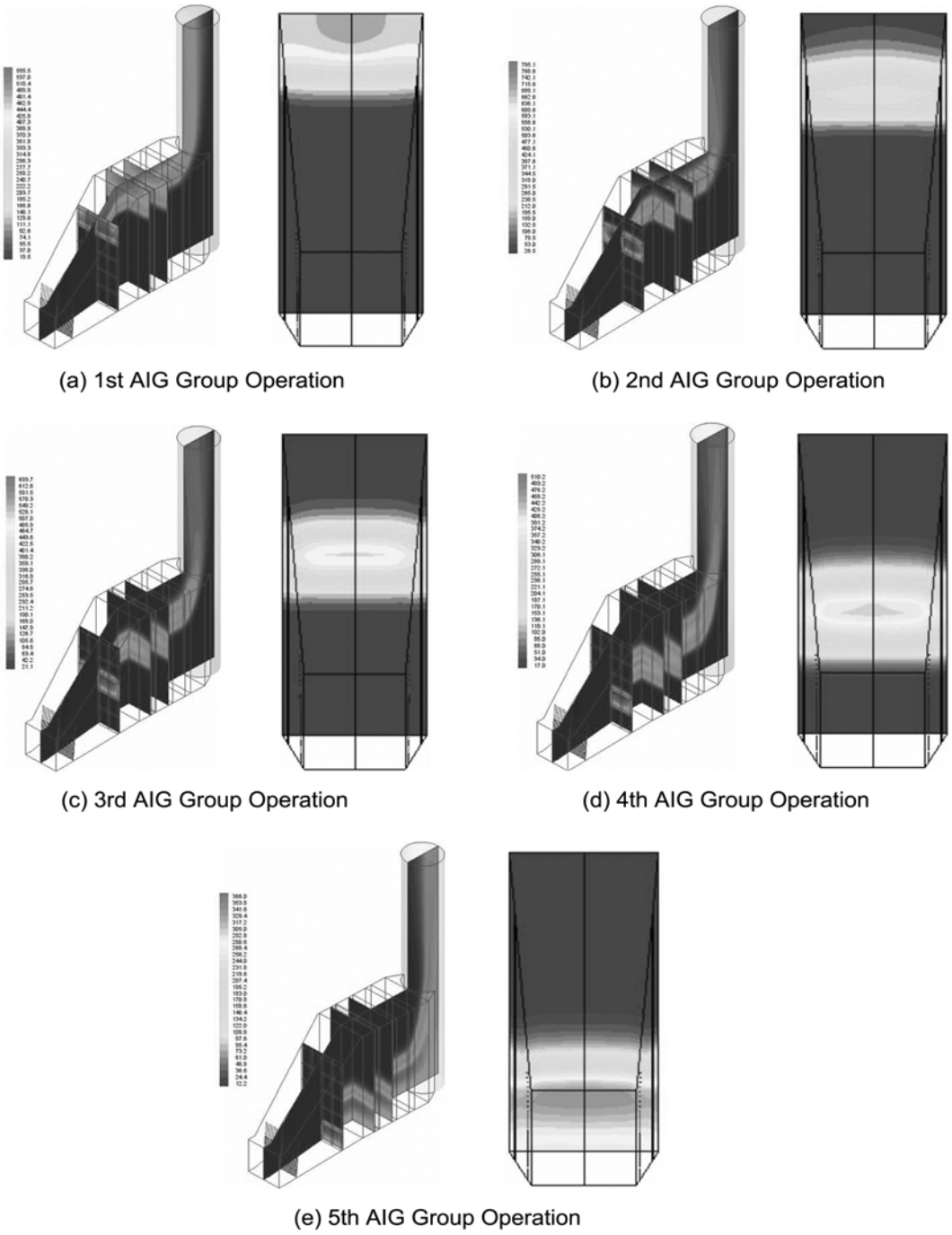

Fig. 13. CFD analysis results of NH_3 concentration distribution for individual AIG group operation, C_v=0.5C_h: (left) total region; (right) 1st catalyst layer.

Table 3. Summary of experimental and CFD analytical results in case of individual AIG group operation

Operating AIG group	Experiment					CFD Analysis	
	Inlet NOx (ppm)	Outlet NOx (ppm)	NOx removal efficiency (%)	NH_3 slip (ppm)	NH_3/NOx	ρV_x at AIG (kg/m^2·sec)	D_c at 1st catalyst layer (%)
1st Group	74.0	61.5	16.9	21.6	0.54	10.02	140.7
2nd Group	79.8	65.4	18.1	11.3	0.48	7.07	128.8
3rd Group	78.9	60.5	23.5	12.9	0.49	8.97	128.3
4th Group	77.4	56.1	27.6	10.8	0.52	11.52	121.2
5th Group	75.9	53.5	29.6	7.9	0.50	15.91	121.5

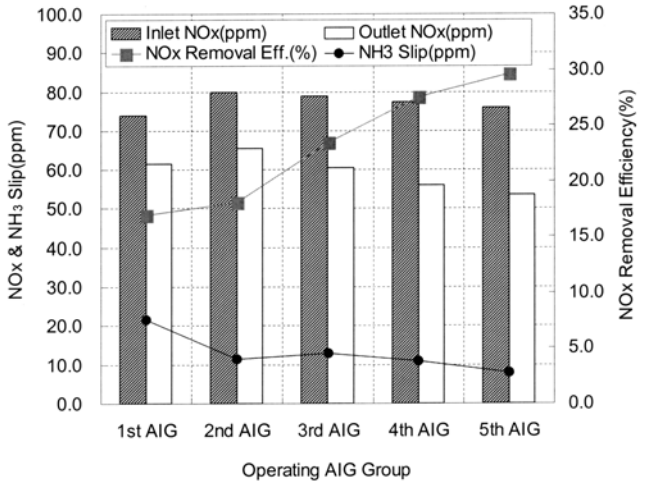

Fig. 14. Performance test result for individual AIG group operation: (▨) inlet NOx (ppm); (□) outlet NOx (ppm); (■) NOx removal efficiency (%); (○) NH_3 slip (ppm).

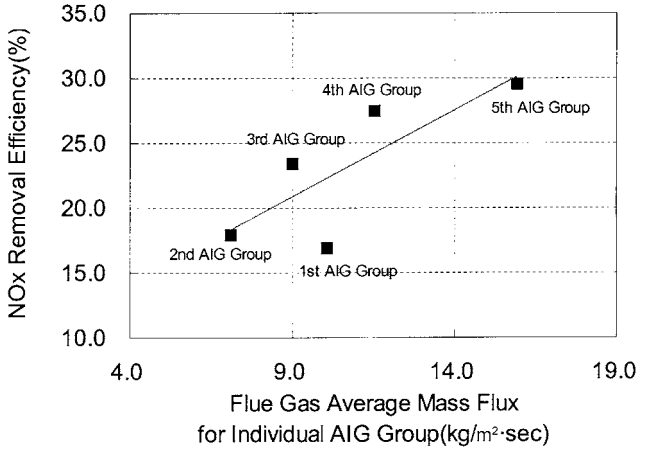

Fig. 16. Relationship between flue gas average mass flux, ρV_x and NOx removal efficiency for individual AIG group operation.

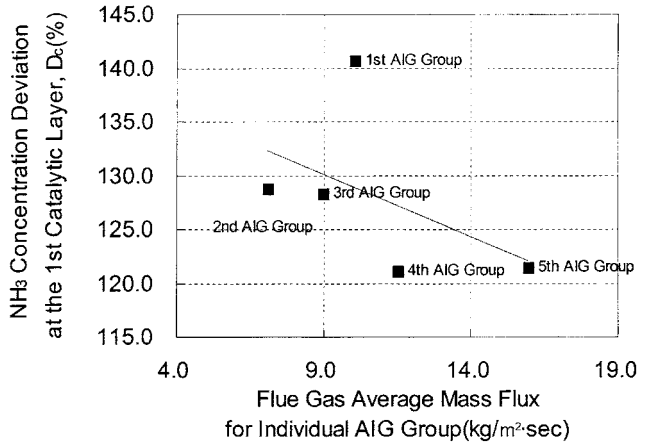

Fig. 15. Relationship between flue gas average mass flux, ρV_x at individual AIG group and NH_3 concentration deviation, D_c at the 1st catalyst layer for individual AIG group operation.

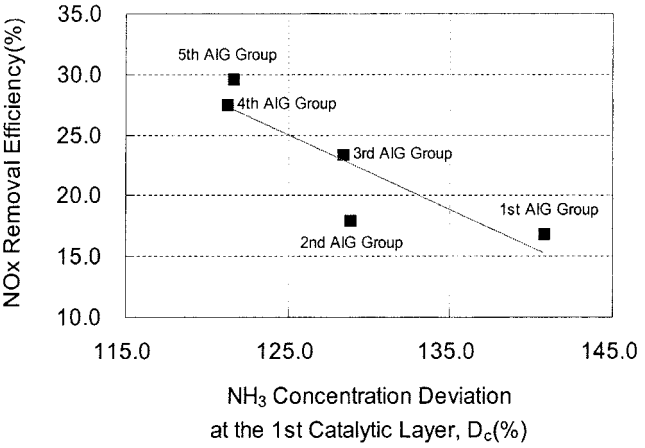

Fig. 17. Relationship between NH_3 concentration deviation, D_c at the 1st catalyst layer and NOx removal efficiency for individual AIG group operation.

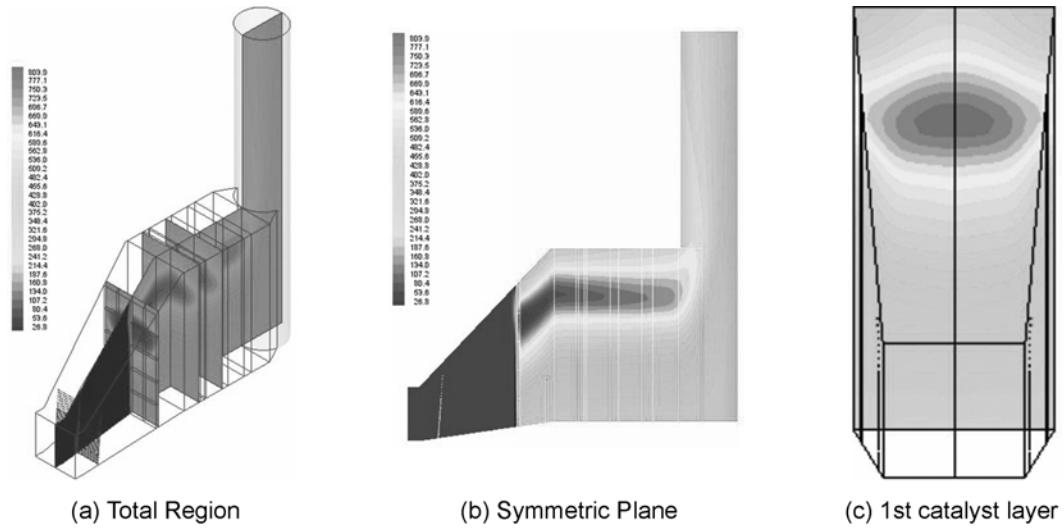

Fig. 18. CFD analysis result of NH_3 concentration distribution for performance test of CASE1, C_v=0.5C_h.

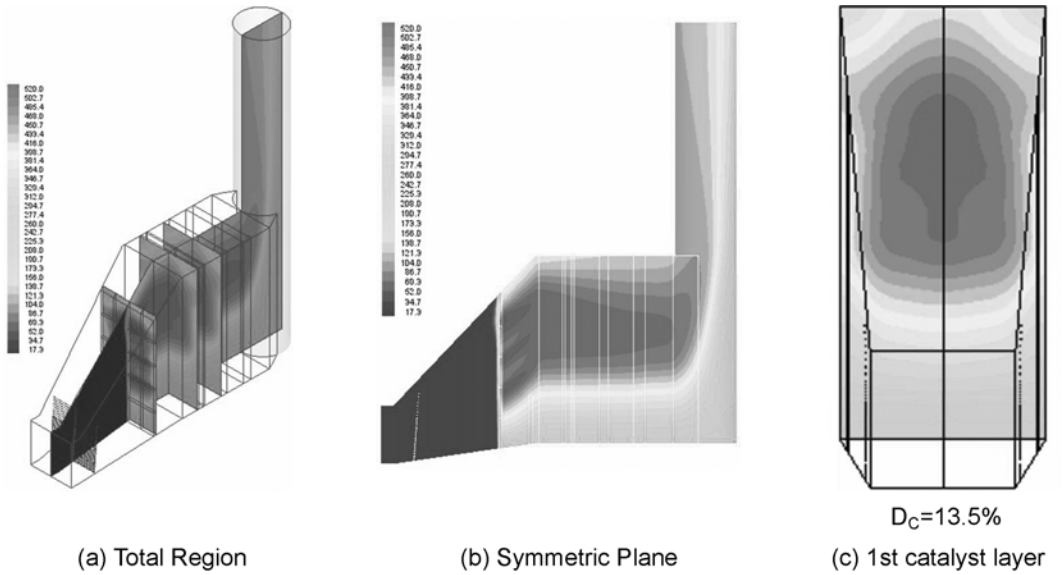

Fig. 19. CFD analysis result of NH_3 concentration distribution for performance test of CASE2, C_v=0.5C_h.

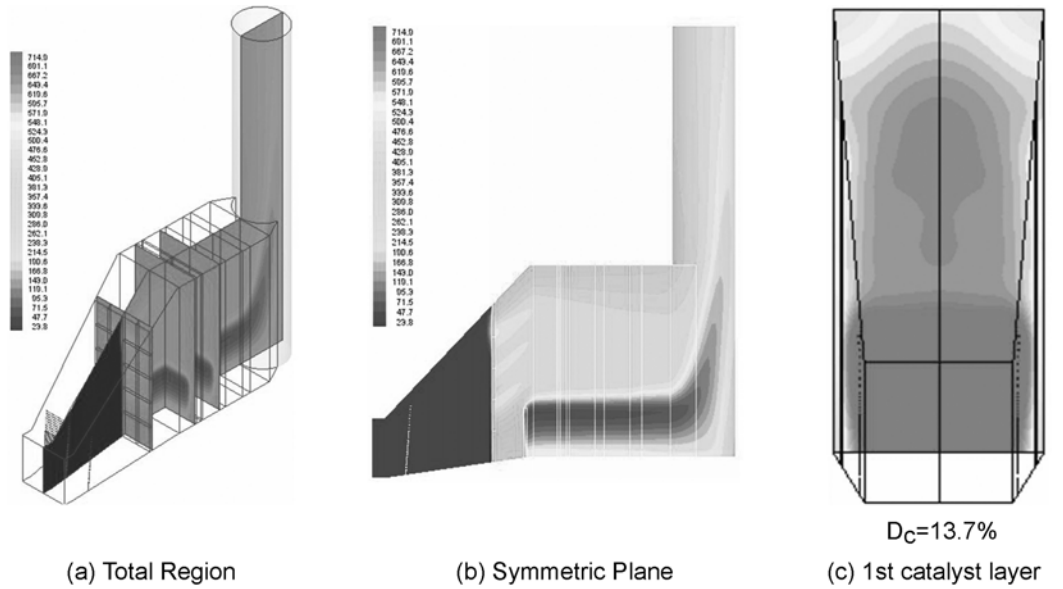

Fig. 20. CFD analysis result of NH_3 concentration distribution for performance test of CASE3, C_v=0.5C_h.

catalyst area and most of the NH_3 injected can react with NOx. If NH_3 is injected at the region, in which flue gas mass flux is low, the flue gas mixing amount between the flue gas with NH_3 and the flue gas without NH_3 will be reduced and it makes available catalyst area decreased and much of NH_3 should flow out without NOx reduction reaction. In addition, the extent of upward movement of flue gas in the upper part of HRSG is slight because of the ceiling. Thus, it is difficult to expect the flue gas mixing effect by rising movement of flue gas just as 4^{th} and 5^{th} AIG group operations in 1^{st} AIG group operation.

The results of performance tests in individual AIG group operation and CFD analysis show that there is flue gas mass flux deviation in the inlet expansion duct of horizontal HRSG. Moreover, NH_3 concentration deviation at the catalyst layer, available catalyst area and NOx removal efficiency can be changed by flue gas mass flux at the NH_3 injection position. Therefore, it is concluded that NH_3 feed rates for individual AIG groups should be determined in proportion to flue gas mass fluxes passing through individual AIG groups in order to maximize the performance of commercial scale SCR.

3. Performance Test Using All AIG Groups

CFD analysis results for NH_3 concentration distribution inside HRSG are shown in Fig. 18, 19, 20 and 21. Table 4 and Fig. 22 are a summary of experimental results and NH_3 concentration deviation, D_c at the 1^{st} catalyst layer from CFD analysis for all cases. In CASE1, D_c at the 1^{st} catalyst layer was 23.6%, which was the highest value out of all cases. NOx removal efficiency in performance test was 54.4%. Average NH_3 slip was 10.0 ppm during the experiment because SCR operation was done under constant NH_3 slip, 10.0 ppm. Total NH_3 average feed rate and NH_3/NOx molar ratio is 46.4 Nm^3/hr and 0.565, which is the lowest value out of all cases. It is inter-

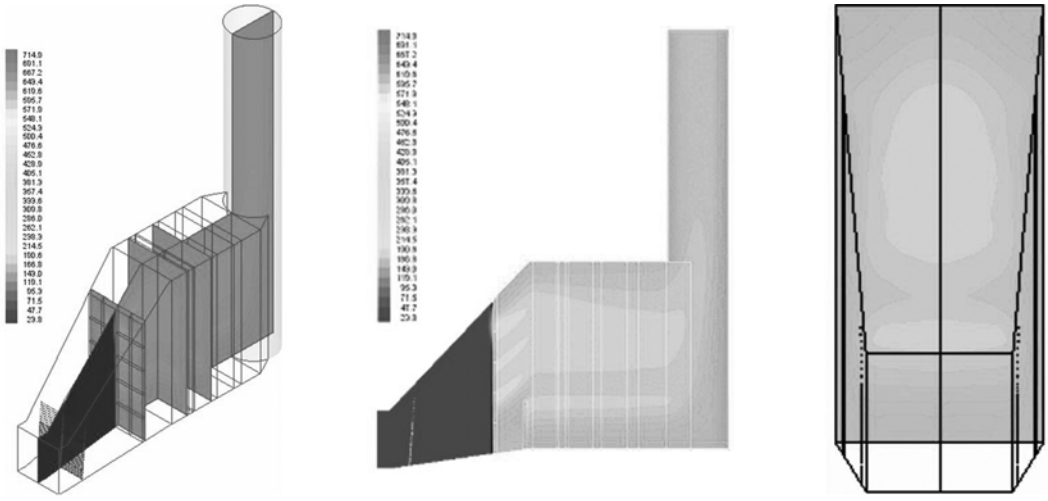

Fig. 21. CFD analysis result of NH_3 concentration distribution for performance test of CASE4, $C_v=0.5C_h$.

Table 4. Summary of experimental and CFD analytical results in case of all AIG groups operation

CASE	Experiment						CFD analysis
	Inlet NOx (ppm)	Outlet NOx (ppm)	NOx removal efficiency (%)	NH_3 slip (ppm)	NH_3 feedrate (Nm^3/hr)	NH_3/NOx	D_c at 1st catalyst layer (%)
CASE1-1	114.8	53.5	53.4	10.0	48.6	0.54	23.6
CASE1-2	94.6	42.3	55.4	10.0	44.1	0.59	
CASE1 average	104.7	47.9	54.4	10.0	46.4	0.57	
CASE2-1	88.8	24.7	72.3	10.0	58.9	0.84	13.5
CASE2-2	98.4	30.1	69.2	10.2	60.8	0.80	
CASE2 average	93.6	27.4	70.8	10.1	59.8	0.82	
CASE3-1	79.4	31.8	60.0	10.1	48.9	0.78	13.7
CASE3-2	102.4	42.2	58.9	10.1	51.4	0.64	
CASE3 average	90.9	37.0	59.4	10.1	50.1	0.71	
CASE4-1	97.2	24.6	74.7	10.1	66.9	0.89	8.6
CASE4-2	99.6	24.9	75.0	10.1	64.1	0.81	
CASE4 average	98.4	24.8	74.8	10.1	65.5	0.85	

preted that there is excessive NH_3 in upper catalyst layer and insufficient NH_3 in the low catalyst layer because the same amount of NH_3 for all AIG groups was injected without regard for flue gas mass flux deviation. D_c at the 1st catalyst layer in CASE2 was 13.5% and NOx removal efficiency was 70.8%. NH_3 slip at the stack was 10.1 ppm. Total NH_3 average feed rate was 59.8 Nm^3/hr and NH_3/NOx molar ratio was 0.815. The operation results of CASE2 were more improved than those of CASE1. However, it seems that NH_3 was deficient in the low part of HRSG as shown in Fig. 18. In CASE3, the 6th AIG group operation was introduced in order to solve the CASE2's problem. D_c at the catalyst layer is similar with CASE2 as 13.7% but NOx removal efficiency was 59.4% under NH_3 slip of 10.1 ppm. Total NH_3 average feed rate was 50.1 Nm^3/hr and NH_3/NOx molar ratio was 0.708, which are less than those of CASE2. It seems that NH_3 injected through the 6th AIG group brought about excessive NH_3 in the lower part of catalyst layer and the excessive NH_3 led to increase NH_3 slip rapidly. Because it was necessary to find the optimal NH_3 feed rate of the 6th AIG group in order to solve this problem, NH_3 feed rate of the 6th AIG group in CASE4 was reduced to 33% of that in CASE3. In CASE4, D_c was 8.6% and NOx removal efficiency was 74.8%, which was the highest value among all cases. NH_3 slip was 10.1 ppm. Total NH_3 average feed rate was 65.5 Nm^3/hr and NH_3/NOx molar ratio was 0.852. It means that NH_3 deficiency or excess phenomena in the low part of catalyst layer in CASE2 and CASE3 were relieved.

From the results of performance test in all AIG groups operation and CFD analysis, D_c can be regulated by adjusting NH_3 injection amounts for individual AIG groups, that is, NH_3 concentration distribution can be homogeneous by means of injecting NH_3 corresponding with flue gas mass flux. As shown in Fig. 23, NOx removal efficiency was increased as D_c at the catalyst layer became decreased. Therefore, it is concluded that NH_3 injection amounts for individ-

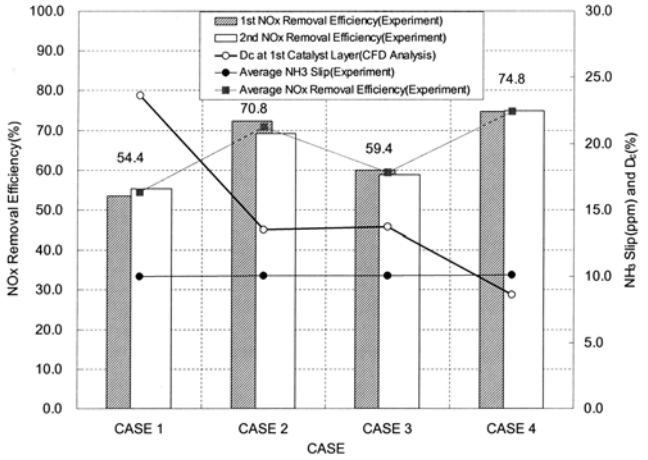

Fig. 22. Operating results for all AIG groups operation: (▨) NOx removal efficiency (1st experiment); (□) NOx removal efficiency (2nd experiment); (■) average NOx removal efficiency; (●) D_c at 1st catalyst layer (CFD analysis); (○) average NH_3 slip (experiment).

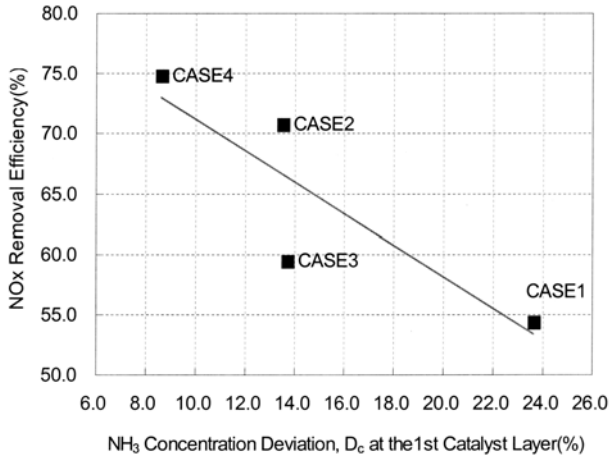

Fig. 23. Relationship between D_c at the 1st catalyst layer and NOx removal efficiency for all AIG groups operation.

ual AIG groups should be determined in accordance with flue gas mass flux passing through AIG in order to improve NOx removal efficiency. And CFD analysis method makes it possible to determine the optimal NH_3 feed rates for individual AIG groups easily.

CONCLUSIONS

CFD analysis for commercial scale SCR installed in horizontal HRSG of combined cycle power plant was implemented. NH_3 injection method which could increase NOx removal efficiency was suggested and applied to real operations. The following conclusions were obtained from CFD analysis and experimental results.

Flue gas behavior inside HRSG was verified by using CFD analysis assuming that heat transfer pipe bundles are porous media. Primarily, flue gas behavior is corrected during passing through the existing flow correction device. However, flue gas distribution in the AIG region is still not even and most of flue gas flows through the low part of HRSG. In front of HPSH, strong upward movement of flue gas occurs. Downstream of HPSH, flue gas behavior becomes very uniform.

As a result of applying different vertical resistance coefficients, it is proved that the porous media assumption is very effective in CFD analysis on HRSG and SCR. The flue gas and NH_3 concentration distribution at AIG and catalyst layer are quantified by using flue gas mass flux deviation, D_m and NH_3 concentration deviation, D_c.

From the experimental results, it was established that NH_3 injection corresponding with flue gas mass flux passing through AIG made it possible to form a homogeneous NH_3 concentration distribution at the catalyst layer and a uniform NH_3 concentration distribution at the catalyst layer contributed to improve the performance of commercial scale SCR. Computational fluid dynamics analysis method is very useful to determine the optimal NH_3 injection amounts for individual AIG groups which make NOx removal efficiency improved.

Finally, CFD analysis method can be applied to determine the optimal location of AIG and catalyst layer in case of the combined cycle power plant in which SCR catalyst and AIG should be installed inside the existing HRSG without additional SCR reactor. It is also expected that improved NOx removal efficiency can be obtained by applying different NH_3 feed rates for individual AIG groups based on flue gas mass flux (verified CFD analysis) if AIG should be installed where flue gas behavior is not uniform. Furthermore, it is expected that time and effort can be saved for system tuning and test operation.

ACKNOWLEDGMENTS

The authors would like to thank the Korea Energy Management Corporation (KEMCO) for the financial support of this project (2001-C-CT06-P-01-0-000-2002).

NOMENCLATURE

t : time
x_j : jth coordinate (if j=1 x, if j=2 y, if j=3 z)
u_j : j direction velocity
S_m : mass source term
p : pressure
g_j : acceleration of gravity
F_j : momentum source term
S_ϕ : source of ϕ
$\overline{w}$: average velocity of main flow direction
$\overline{c}$: average NH_3 concentration
D : viscous resistance coefficient
C : inertial resistance coefficient
T : porous media thickness
K_L' : real resistance coefficient of porous media
A : cross section area by opening
D_m : flue gas mass flux distribution deviation parameter
D_c : NH_3 concentration distribution deviation parameter

Greek Letters

ρ : density
μ : kinematic viscosity of fluid

ϕ : scholar variable
Γ : diffusion coefficient
α : permeability [m^2]

REFERENCES

Adams, B., Cremer, M., Valentine, J., Bhamidipati, V., Letcavits, J., O'Connor, D. and Vierstra, S., *Use of CFD modeling for design of NOx reduction systems in utility boilers*, Proceeding of the 2002 International Joint Power Generation Conference, ASME, Phoenix, AZ (2002).

Arbind, P., "Air pollution control technologies for nitrogen oxides," *The National Environmental Journal*, **46**, May (1995).

Bruce, I., "NOx reduction techniques," *The American Ceramic Society Bulletin*, **81**, Oct. (1995).

Fluent User's Guide, Version 6.1; Fluent: Lebanon, NH (1998).

Freek, K., Lydia, S., Nico, J. J. D. and Jacob, A. M., "Kinetics of the selective catalyst reduction of NO with NH_3 over Mn_2O_3,-WO_3/-Al_2O_3," *Ind. Eng. Chem. Res.*, **445**, 32 (1993).

Heck, R. M., Chen, J. M. and Speronello, B. K., "Operating characteristics and commercial operating experience with high temperature SCR NOx catalyst," *Environmental Progress*, **221**, 13 (1994).

Jaime, B., *Progress engineering and design for air pollution control*, Prentice Hall, New Jersey (1993).

Jiri, S., Natale, F., Pio, F., Enrico, T. and Fiorenzo, B., "Selective reduction of NOx by NH_3 over honeycomb DeNOxing catalysts," *Ind. Eng. Chem. Res.*, **1053**, 32 (1993).

Kenneth, J. F. and John, H. C., "Design guidelines for NH_3 injection grids; optimize SCR NOx removal," *Oil & Gas Journal*, **56**, Nov. (1993).

Kevin, R., Mel, A. and Michael, V., *Numerical modeling for design optimization of SCR applications*, ICAC NOx Forum Washington D.C. (2000).

Kevin, R., Milobowski, M. and Wooldridge, B., *Perspectives on ammonia injection and gaseous static mixing in SCR retrofit applications*, EPRI-DOE-EPA Combined Utility Air Pollutant Control Symposium, Washington D.C. (1999).

Kokkinos, A., Nelson, N. and Stirgwolt, W., *Structural considerations for SCR retrofits*, EPRI-DOE-EPA Combined Utility Air Pollutant Control Symposium, Washington D.C. (1999).

Kotter, M. and Lintz, H. G., "Selective catalyst reduction of nitrogen oxides - an original concept," *International Chemical Engineering*, **685**, 31 (1991).

Launder, B. E. and Spalding, D. B., *Mathematical models of turbulence*, Academic Press, London, England (1972).

Pantankar, S. V., *Numerical heat transfer and fluid flow*, Hemisphere Publishing Corporation, Washington D.C. (1980).

Ralf, S., Cindy, K. and Edward, H., "Enhance ammonia distribution for maximum SCR performance," *Institute of Clean Air Companies Forum 2003*, **4**, Oct. (2003).

Sayre, A. and Milobowski, M., *Validation of numerical models of flow through SCR units*, EPRI-DOE-EPA Combined Utility Air Pollutant Control Symposium, Washington D.C. (1999).